Timing and Frequency Offsets Compensation in Relay Transmission for 3GPP LTE Uplink

Conference Paper · May 2010

DOI: 10.1109/ICC.2010.5502765 · Source: DBLP

This full text paper was peer reviewed at the direction of IEEE Communications Society subject matter experts for publication in the IEEE ICC 2010 proceedings

Timing and Frequency Offsets Compensation in Relay Transmission for 3GPP LTE Uplink

Animesh Yadav, Visa Tapio, Markku Juntti and Juha Karjalainen
Centre for Wireless Communication
P.O.Box 4500 FI-90014
University of Oulu, Finland
Email: {animesh.yadav, visa.tapio, markku.juntti, juha.karjalainen}@ee.oulu.fi

***Abstract*—Relays can be used between the source and the destination to improve network coverage or reliability. In the relay based distributed space-time block-coded (DSTBC) single-carrier (SC) transmission scheme, asynchronism in time and frequency causes degradation in system performance because of the interblock interference, non-coherent combining and multiuser interference. The simultaneous presence of timing offset and carrier frequency offset also destroy the orthogonal structure of DSTBC. In this paper, we study the combined effect of timing offset and carrier frequency offset and propose a two stage equalization technique for this system at the destination terminal. Technique is based on interference cancellation and cyclic prefix reconstruction. The proposed equalization technique maintains the orthogonal structure of DSTBC and allows the use of low complexity one-tap frequency-domain equalizer. The technique significantly alleviates the effect of time offsets and frequency offsets at the destination without increasing the complexity of the receiver or disturbing the 3^{rd} generation partnership project-long term evolution (3GPP LTE) uplink frame structure or the data rate over frequency selective channels.**

I. Introduction

Use of single-carrier (SC) transmission scheme has been standardized in the 3^{rd} Generation Partnership Project-Long Term Evolution (3GPP LTE) uplink [1]. The single-carrier transmission scheme combined with minimum mean-square error frequency-domain equalization (SC MMSE-FDE) is well suited at the mobile side because of its simple structure and low peak-to-average power ratio (PAPR) [2]. SC MMSE-FDE has low complexity, due to its use of computationally-efficient fast Fourier transform (FFT), than time-domain equalization whose complexity grows exponentially with channel memory and spectral efficiency [3], [4].

Space-time block coding (STBC) [5] is an effective technique to exploit spatial diversity not only in multiple-input multiple-output (MIMO) communications but also in co-operative communications [6]. Most of the existing studies on co-operative transmission assume perfect synchronization between the co-operative users and the relays, which means that the timings, carrier frequencies, and propagation delays are identical for the user and the relay [7], [8], [9]. However, such perfect synchronization between the user and the relay is difficult because of their different locations, their independent mobility and local oscillators, which do not share a timing reference.

In general, interblock interference (IBI) occurs at the destination due to frequency selectivity of the channels and timing offset (TO) between transmitting and receiving terminals. Intercarrier interference (ICI) and multi-user interference (MUI) occur due to imperfect carrier synchronization between the source and the destination. For relay based single user SC systems, carrier frequency offsets (CFO) between the source-to-destination and the relay-to-destination will result in non-coherent combining of the signals at the destination terminal. If the transmission uses STBC, simultaneous presence of TO and CFO destroy the orthogonal structure of STBC, thereby causing conventional decoding to fail.

In co-operative wireless systems, timing offset (TO) occurs due to different relative propagation delay values between the signals from the source to the destination and from the relay to the destination. TO can be easily compensated for by utilizing a large cyclic prefix (CP) in the wireless system but a large CP, on the other hand, decreases spectral efficiency. In practice, CP will not be sufficient to compensate for TO when the sum of the multipath delay spread and the relative propagation delay is larger than the CP length. We have partially addressed the problem of the presence of TO in a relay based system [10], where we have proposed an equalization scheme based on interblock interference cancelation (IBIC) and cyclic prefix reconstruction (CPR).

Carrier frequency offsets (CFO) occurs due to different oscillator frequencies at the source and at the relay w.r.t. the destination, and due to Doppler shift caused by source mobility. The use of a master synchronization beacon at the destination terminal has been proposed to mitigate the effect of CFO in co-operative/relay based system, [11], [12], [13]. The destination terminal sends back the frequency offset information to the co-operative transmitters for pre-compensation. Shen *et al.* [14] have proposed a linear minimum mean-square error (LMMSE) detector to detect the STBC coded data under multiple CFOs. A novel minimum mean-square error (MMSE) decision feedback equalizer (DFE) that explicitly accounts for the frequency offsets at the receiver has been proposed in [15]. A Viterbi equalizer is proposed in [16] for cooperative diversity in CFO.

A very different approach from others, [17] proposed a double-differential modulation, which requires no channel

This research has been supported by Tekes, the Finnish Funding Agency for Technology and Innovation, Elektrobit Group, Nokia, Nokia Siemens Networks, Texas Instruments, Uninord, and Tauno Tönningin Säätiöstä.

gains or carrier offsets to decode the data, for cooperative wireless system to improve the performance with random carrier offsets. In [18], authors have proposed to compensate the multiple CFOs by modifying space-frequency block-code (SFBC), minimum Euclidean distance decision criterion and interference reconstructing eliminator.

In this paper, we propose a novel equalization scheme that compensates TO and CFOs simultaneously and allows the use of low complexity MMSE-FDE for SC-DSTBC transmission scheme. To the best of our knowledge, this is the first attempt to investigate the effect of asynchronism in the SC-DSTBC transmission scenario. In this work, we have assumed that source has mobility and the sum of multipath delay spread and relative propagation delay is larger than the CP length. Amplify-and-forward (AF) relaying protocol which is the simplest class of co-operative communication protocols [19] is used at the relay terminal. It is shown through simulation that if the perfect estimate of TO, CFOs, and channel impulse response are known at the receiver, the proposed equalizer can reduce the effect of TO and CFOs significantly.

Notations: $(\cdot)^*, (\cdot)^T$ and $(\cdot)^H$ denote conjugate, transpose, and Hermitian transpose operations, respectively. $\otimes$ denotes Kronecker product, $[\cdot]_{k,l}$ denotes the $(k,l)^{th}$ entry of a matrix, $[\cdot]_k$ denotes the $(k)^{th}$ entry of a vector. $\mathbf{I}_N$ denotes the identity matrix of size N. $\mathbf{0}_{M\times M}$ denotes all-zero matrix of size $M \times M$, diag($\mathbf{v}$) stands for a diagonal matrix with vector $\mathbf{v}$ on its diagonal, and $\mathbf{F}_N$ represents the $N \times N$ fast fourier transform (FFT) matrix whose (l,k) elements is given by $\mathbf{F}_N(l,k) = (1/\sqrt{N})\exp(-j2\pi lk/N)$ where $0 \le l, k \le N-1$. We define a set of $N \times N$ permutation matrices $\{\mathbf{P}\}$ and $\{\mathbf{R}_\tau\}$ that performs a reversed cyclic shift and a cyclic shift respectively, i.e., for a vector $\mathbf{a} = [a_0 \cdots a_{N-1}]^T$, $[\mathbf{Pa}]_n = \mathbf{a}_{(-n \bmod N)}$ and $[\mathbf{R}_\tau \mathbf{a}]_s = \mathbf{a}_{(s-\tau) \bmod N}$. $\mathbf{R}_\tau = \mathbf{F}_M^H \mathbf{D}_\tau \mathbf{F}_M$, where $\mathbf{R}_\tau$ = diag($[\mathbf{F}_M]_{0:M-1,\tau}\sqrt{M}$). Bold upper-case letters denote matrices and bold lower-case letters denote vectors.

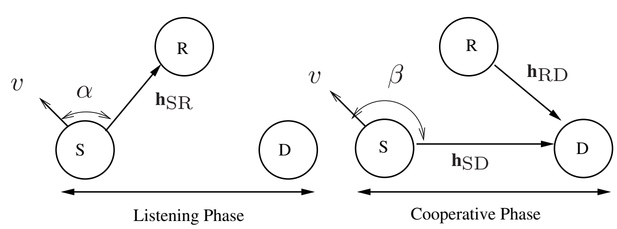

Fig. 1. Illustration of the DSTBC SC MMSE-FDE protocol.

II. System Model

A. 3GPP-LTE Co-operative Uplink

Consider an amplify-and-forward (AF) relay based DSTBC transmission scheme for SC MMSE-FDE 3GPP LTE uplink. In Fig. 1, a co-operative system is shown with one moving source (S) terminal, one fixed relay (R) terminal and one fixed destination (D) terminal. All terminals are equipped with a single transmit and receive antenna. The user co-operation protocol III proposed by Nabar *et al.* [20], [21] is adopted: Each transmission has two signaling phases, the first called the listening phase in which the source terminal communicates with the relay terminal. There is no direct transmission from the source to the destination terminal during this period. The second phase is called the co-operation phase, in which both the relay and the source terminals communicate with the destination terminal. For the link between the relay and the destination, AF relaying is used, in which the relay terminal amplifies and retransmits the signal received from the source terminal in the listening phase. The 3GPP LTE uplink supports quadrature phase shift keying (QPSK), M-ary modulation techniques such as quadrature amplitude modulation (QAM), 16-QAM and 64-QAM.

The effect of TO and CFO can be seen during co-operation phase and compensating the same at the destination in the relay based wireless systems is a complex problem. In this paper we will study this problem and propose a solution to compensate both TO and CFOs.

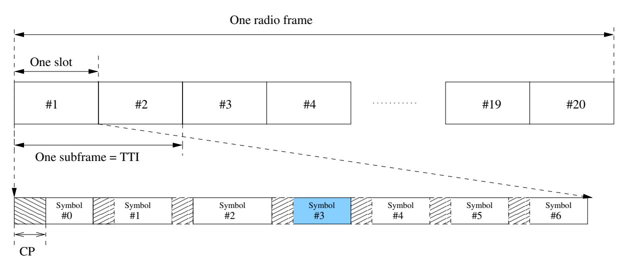

Fig. 2. 3GPP-LTE frame structure.

The 3GPP LTE uplink frame structure is shown in Fig. 2 Each uplink radio frame is of 10 ms duration and consists of 20 slots each of 0.5 ms duration. And each slot is made up of 6 symbols consisting of 5 physical uplink shared channel (PUSCH) data symbols and 1 reference symbol in the middle. Two slots form one subframe which is also called as transmission time interval (TTI). Each TTI has 12 data symbols and 2 reference symbols and all are cyclic prefixed with length L_{cp} to remove IBI and to make channel matrices circulant.

The sum of multipath delay spread and propagation delay is assumed to be larger than the CP length. The source is moving with velocity v while all terminals oscillators are locked to the same frequency. CFOs in the system is solely because of Doppler shift in the frequencies received at the relay and the destination. Because of TO, IBI takes place between symbols within the TTI and the circulant structure of the channel matrix gets destroyed. Moreover, due to CFOs in the cooperation phase, signals received from the relay and the source combine non-coherently at the destination. It causes problems during decoupling the symbols during DSTBC decoding. In DSTBC decoding, the undesired symbol acts as interference for the desired symbol being estimated.

B. Signal Model

Assume that all underlying links experience frequency selective fading. The channel impulse response (CIR) for the j^{th} transmission is given by $\mathbf{h}_{\mathrm{AB}} = [h^j_{\mathrm{AB}}(0), h^j_{\mathrm{AB}}(1), \cdots, h^j_{\mathrm{AB}}(L_{\mathrm{AB}})]$, where L_{AB} is the channel memory length and $\mathbf{H}^j_{\mathrm{AB}} \in \mathbb{C}^{N\times N}$ is the corresponding channel convolution matrix corresponding to link A→B. $\tilde{\Gamma}_{\mathrm{AB}} \in \mathbb{C}^{M\times M}$ is a diagonal matrix with $[\tilde{\Gamma}_{\mathrm{AB}}]_{k,k} = e^{j2\pi\Delta f_{\mathrm{AB}}k/M}$ and $\Gamma_{\mathrm{AB}} \in \mathbb{C}^{N\times N}$ is a diagonal matrix such that $\Gamma_{\mathrm{AB}} = \mathbf{I}_{N/M} \otimes \tilde{\Gamma}_{\mathrm{AB}}$, where Δf_{AB} is a CFO between link A→B normalized by f_{SC}/M and f_{SC} is system bandwidth. The subscript (AB) can be source-to-relay (SR), relay-to-destination (RD) or source-to-destination (SD). The CIRs for all links vary independently for every link and are assumed to be constant over two transmissions.

Two consecutive TTIs, $\mathbf{s}_1^j = [\mathbf{x}_1^{j^T}(0), \ldots, \mathbf{x}_1^{j^T}(13)]^T \in \mathbb{C}^N$ and $\mathbf{s}_2^j = [\mathbf{x}_2^{j^T}(0), \ldots, \mathbf{x}_2^{j^T}(13)]^T \in \mathbb{C}^N$, where $N = 14(M + L_{\mathrm{cp}})$ is the length of a TTI, M is the length of a PUSCH data symbol x belongs to the uplink frame as shown in Fig. 2 are sent in every j^{th} transmission. The input symbols are assumed to complex, zero-mean, and uncorrelated with variance σ_x^2.

Source is moving with velocity v. Forward velocity of the source makes an angle α with the line-of-sight from itself to the relay terminal as shown in Fig. 1. Due to the Doppler effect, carrier frequency shift will be observed at the relay terminal. The received signal vector $\mathbf{r}_{\mathrm{R}}^j \in \mathbb{C}^N$ at the relay during the listening phase is given by

$$\mathbf{r}_{\mathrm{R}}^j = \Gamma_{\mathrm{SR}}\mathbf{H}_{\mathrm{SR}}^j\mathbf{s}_1^j + \mathbf{n}_{\mathrm{R}}^j, \tag{1}$$

where $\mathbf{n}_R^j \in \mathbb{C}^N$ is the additive white Gaussian noise (AWGN) vector at the relay with each entry having zero-mean and variance σ_n^2. For convenience, all noise variance are assumed equal to σ_n^2.

In the second transmission time interval, because of TO, the signal from the source terminal arrives at the destination terminal τ samples later than the signal from the relay terminal. The timing errors will cause τ samples shift between the signals from the source and the relay terminals. Forward velocity of the source makes an angle β with the line-of-sight from itself to the destination terminal as shown in Fig. 1. The destination terminal will observe a carrier frequency shift because of Doppler shift in the frequency of the signal received from the source. Assume that the amplifying factor at the relay terminal is unity. Therefore, the received vector $\mathbf{r}_D^j \in \mathbb{C}^N$ at the destination terminal in the co-operative phase is given by

$$\mathbf{r}_{\mathrm{D}}^j = \rho\mathbf{H}_{\mathrm{RD}}^j\mathbf{r}_{\mathrm{R}}^j + \Gamma_{\mathrm{SD}}\mathbf{R}_\tau\mathbf{H}_{\mathrm{SD}}^j\mathbf{s}_2^j + \mathbf{n}_{\mathrm{D}}^j, \tag{2}$$

where $\mathbf{n}_{\mathrm{D}}^j \in \mathbb{C}^N$ is an AWGN vector at the destination and ρ is a constant amplification factor that maintains the average energy of the signal transmitted from the relay terminal equal to σ_x^2. Assume that the both the source terminal and the relay terminal transmit with equal power.

Finally, combining (1) and (2), we obtain,

$$\mathbf{r}_{\mathrm{D}}^j = \rho\mathbf{H}_{\mathrm{RD}}^j\Gamma_{\mathrm{SR}}\mathbf{H}_{\mathrm{SR}}^j\mathbf{s}_1^j(n) + \Gamma_{\mathrm{SD}}\mathbf{R}_\tau\mathbf{H}_{\mathrm{SD}}^j\mathbf{s}_2^j(n) + \bar{\mathbf{n}}_{\mathrm{D}}^j, \tag{3}$$

where we define the effective noise term $\bar{\mathbf{n}}_{\mathrm{D}}^j \in \mathbb{C}^N$ at the destination as

$$\bar{\mathbf{n}}_{\mathrm{D}}^j = \rho\mathbf{H}_{\mathrm{RD}}^j\mathbf{n}_{\mathrm{R}}^j + \mathbf{n}_{\mathrm{D}}^j. \tag{4}$$

In the $(j+1)^{th}$ transmission interval, $\bar{\mathbf{s}}_2^{j+1} = [-\mathbf{P}\mathbf{x}_2^{*j^T}(0), \ldots, -\mathbf{P}\mathbf{x}_2^{*j^T}(13)]^T$ is transmitted from the source to the relay terminal and $\bar{\mathbf{s}}_1^{j+1} = [\mathbf{P}\mathbf{x}_1^{*j^T}(0), \ldots, \mathbf{P}\mathbf{x}_1^{*j^T}(13)]^T$ is transmitted from source to the destination terminals. This transmission has time reversed (TR) PUSCH data symbols which help in STBC decoding as can be seen later. We assume that Δf_{AB}, τ, and channel matrix $\mathbf{H}_{\mathrm{AB}}^j$ remain constant over the j^{th} and $(j+1)^{th}$ transmission but random and independent from TTI to TTI. Thus, the received vector $\mathbf{r}_{\mathrm{R}}^{j+1} \in \mathbb{C}^N$ at the relay during the listening phase is

$$\mathbf{r}_{\mathrm{R}}^{j+1} = \Gamma_{\mathrm{SR}}\mathbf{H}_{\mathrm{SR}}^j\bar{\mathbf{s}}_2^{j+1} + \mathbf{n}_{\mathrm{R}}^{j+1}, \tag{5}$$

and the received vector $\mathbf{r}_{\mathrm{D}}^{j+1} \in \mathbb{C}^N$ at the destination terminal during co-operative phase is

$$\mathbf{r}_{\mathrm{D}}^{j+1} = \rho\mathbf{H}_{\mathrm{RD}}^j\Gamma_{\mathrm{SR}}\mathbf{H}_{\mathrm{SR}}^j\bar{\mathbf{s}}_2^{j+1} + \Gamma_{\mathrm{SD}}\mathbf{R}_\tau\mathbf{H}_{\mathrm{SD}}^j\bar{\mathbf{s}}_1^{j+1} + \bar{\mathbf{n}}_{\mathrm{D}}^{j+1}, \tag{6}$$

where we define the effective noise term $\bar{\mathbf{n}}_{\mathrm{D}}^{j+1} \in \mathbb{C}^N$ as

$$\bar{\mathbf{n}}_{\mathrm{D}}^{j+1} = \rho\mathbf{H}_{\mathrm{RD}}^j\mathbf{n}_{\mathrm{R}}^{j+1} + \mathbf{n}_{\mathrm{D}}^{j+1}. \tag{7}$$

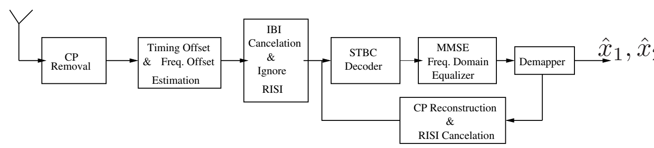

Fig. 3. The proposed receiver.

III. Receiver for Proposed DSTBC SC MMSE-FDE Scheme

The receiver for the proposed DSTBC SC MMSE-FDE system is illustrated in Fig. 3. At the receiver, decoding is performed symbol by symbol. Therefore, the received vector can be rewritten by using (3) and (6) in terms of the data symbols. After removing the CP, we obtain

$$\begin{aligned}\tilde{\mathbf{r}}_{\mathrm{D}}^j \;&=\; \rho\tilde{\mathbf{H}}_{\mathrm{RD}}\tilde{\Gamma}_{\mathrm{SR}}\tilde{\mathbf{H}}_{\mathrm{SR}}\mathbf{x}_1^j(n) + \tilde{\Gamma}_{\mathrm{SD}}\tilde{\mathbf{R}}_\tau\mathbf{H}_{\mathrm{SD}}\mathbf{x}_2^j(n)\\ &\quad+ \tilde{\Gamma}_{\mathrm{SD}}\mathbf{H}_{\mathrm{IBI}}\mathbf{x}_2^j(n-1) + \mathbf{w}_{\mathrm{D}}^j,\end{aligned} \tag{8}$$

and

$$\begin{aligned}\tilde{\mathbf{r}}_{\mathrm{D}}^{j+1} \;&=\; -\rho\tilde{\mathbf{H}}_{\mathrm{RD}}\tilde{\Gamma}_{\mathrm{SR}}\tilde{\mathbf{H}}_{\mathrm{SR}}\mathbf{P}\mathbf{x}_2^{*j}(n) + \tilde{\Gamma}_{\mathrm{SD}}\tilde{\mathbf{R}}_\tau\mathbf{H}_{\mathrm{SD}}\mathbf{P}\mathbf{x}_1^{*j}(n)\\ &\quad+ \tilde{\Gamma}_{\mathrm{SD}}\mathbf{H}_{\mathrm{IBI}}\mathbf{P}\mathbf{x}_1^j(n-1) + \mathbf{w}_{\mathrm{D}}^{j+1},\end{aligned} \tag{9}$$

where $\mathbf{w}_{\mathrm{D}}^j$, $\mathbf{w}_{\mathrm{D}}^{j+1} \in \mathbb{C}^M$ are AWGN vectors, $\tilde{\mathbf{r}}_{\mathrm{D}}^j$, $\tilde{\mathbf{r}}_{\mathrm{D}}^{j+1} \in \mathbb{C}^M$ are the received vectors, $\tilde{\mathbf{H}}_{\mathrm{RD}}$, $\tilde{\mathbf{H}}_{\mathrm{SR}} \in \mathbb{C}^{M\times M}$ are circulant channel matrices for the channel from the relay to the destination and from the source to the relay respectively. $\tilde{\mathbf{R}}_\tau \in \mathbb{C}^{M\times M}$ is a cyclic shift matrix and $\mathbf{H}_{\mathrm{SD}} \in \mathbb{C}^{M\times M}$ is a defective channel matrix given by $\mathbf{H}_{\mathrm{SD}} = \tilde{\mathbf{H}}_{\mathrm{SD}} - \mathbf{H}_{\mathrm{IBI}}$, where $\tilde{\mathbf{H}}_{\mathrm{SD}} \in \mathbb{C}^{M\times M}$ is the circulant channel matrix for the channel from source to destination and $\mathbf{H}_{\mathrm{IBI}} \in \mathbb{C}^{M\times M}$ is an interblock interference matrix. Note that decoding is done only for PUSCH data symbols and not for reference symbols.

At the receiver, STBC decoding to estimate $\mathbf{x}_1^j(n)$ and $\mathbf{x}_2^j(n)$ from $\tilde{\mathbf{r}}_{\mathrm{D}}^j$ and $\tilde{\mathbf{r}}_{\mathrm{D}}^{j+1}$, will turn out to be efficient if we exploit the following properties of circulant matrices [22].

P1). Circulant matrices can be diagonalized by FFT operation

$$\tilde{\mathbf{H}}_{\mathrm{AB}} = \mathbf{F}_M^H\mathbf{D}_{\mathrm{AB}}\mathbf{F}_M \qquad \text{and} \qquad \tilde{\mathbf{H}}_{\mathrm{AB}}^H = \mathbf{F}_M^H\mathbf{D}_{\mathrm{AB}}^*\mathbf{F}_M, \tag{10}$$

where $\tilde{\mathbf{D}}_{\mathrm{AB}} = \mathrm{diag}(\tilde{H}_{\mathrm{AB}}(e^{j0}), \cdots, \tilde{H}_{\mathrm{AB}}(e^{j2\pi(M-1)/M}))$.

P2). Pre and Post-multiplying $\tilde{\mathbf{H}}_{\mathrm{AB}}$ by $\mathbf{P}$ yields $\tilde{\mathbf{H}}_{\mathrm{AB}}^T$

$$\mathbf{P}\tilde{\mathbf{H}}_{\mathrm{AB}}\mathbf{P} = \tilde{\mathbf{H}}_{\mathrm{AB}}^T \quad \text{and} \quad \mathbf{P}\tilde{\mathbf{H}}_{\mathrm{AB}}^*\mathbf{P} = \tilde{\mathbf{H}}_{\mathrm{AB}}^H. \tag{11}$$

The first stage of equalization contains two steps. The one is IBI cancelation, which removes the unwanted IBI in the received vector from the previous data symbol within the TTIs. The last δ samples of the previously estimated data symbol are subtracted from the first δ samples of the current data symbol. Note that in the DSTBC protocol, each link between the source, the relay and the destination is used for only one of the two signaling phases, i.e., when the link between the source and the relay is busy, other links are idle in the listening phase and vice versa in co-operation phase. Therefore, the first data symbol of every received TTI will have no IBI.

Now the received signals after IBI cancelation are given by

$$\bar{\mathbf{r}}_{\mathrm{D}}^j = \rho\tilde{\mathbf{H}}_{\mathrm{RD}}\tilde{\Gamma}_{\mathrm{SR}}\tilde{\mathbf{H}}_{\mathrm{SR}}\mathbf{x}_1^j(n) + \tilde{\Gamma}_{\mathrm{SD}}\tilde{\mathbf{R}}_\tau\mathbf{H}_{\mathrm{SD}}\mathbf{x}_2^j(n) + \mathbf{w}_{\mathrm{D}}^j, \tag{12}$$

$$\bar{\mathbf{r}}_{\mathrm{D}}^{j+1} = -\rho\tilde{\mathbf{H}}_{\mathrm{RD}}\tilde{\Gamma}_{\mathrm{SR}}\tilde{\mathbf{H}}_{\mathrm{SR}}\mathbf{P}\mathbf{x}_2^{*j}(n) + \tilde{\Gamma}_{\mathrm{SD}}\tilde{\mathbf{R}}_\tau\mathbf{H}_{\mathrm{SD}}\mathbf{P}\mathbf{x}_1^{*j}(n) + \mathbf{w}_{\mathrm{D}}^{j+1}, \tag{13}$$

(12) and (13) can be rewritten in frequency domain as (21) and (24) see Appendix for detail. Again writing them in matrix form, we get,

$$\begin{bmatrix} \mathbf{R}_{\mathrm{D}}^j \\ \mathbf{R}_{\mathrm{D}}^{*j+1} \end{bmatrix} = \begin{bmatrix} \rho\tilde{\Phi}_{\mathrm{SD},1}\tilde{\mathbf{D}}_{\mathrm{RD}}\tilde{\Phi}_{\mathrm{SR},1}\tilde{\mathbf{D}}_{\mathrm{SR}} & \tilde{\mathbf{D}}_\tau\tilde{\mathbf{D}}_{\mathrm{SD}} \\ \tilde{\mathbf{D}}_{\mathrm{SD}}^*\tilde{\mathbf{D}}_\tau^* & -\rho\tilde{\Phi}_{\mathrm{SD},2}\tilde{\mathbf{D}}_{\mathrm{RD}}^*\tilde{\Phi}_{\mathrm{RD},2}\tilde{\mathbf{D}}_{\mathrm{SR}}^* \end{bmatrix} \begin{bmatrix} \mathbf{F}\mathbf{x}_1^j(n) \\ \mathbf{F}\mathbf{x}_2^j(n) \end{bmatrix} + \begin{bmatrix} \mathbf{W}_{\mathrm{D}}^j \\ \mathbf{W}_{\mathrm{D}}^{*j+1}) \end{bmatrix}, \tag{14}$$

where $\tilde{\Phi}_{\mathrm{SR},1,2}$ and $\tilde{\Phi}_{\mathrm{SD},1,2}$ are non-diagonal matrices. Their non-diagonal elements are due to non-coherent combining at the destination terminal during co-operation phase. These elements will give rise to a residual intersymbol interference (RISI) between $\mathbf{x}_1(n)$ and $\mathbf{x}_2(n)$ during detection.

In the second step, the interference is ignored by taking only the diagonal elements of $\tilde{\Phi}_{\{\mathrm{SR},1,2\}}$ and $\tilde{\Phi}_{\{\mathrm{SD},1,2\}}$. Since $\tilde{\Phi}_{\{\mathrm{SD},2\}}^{\mathrm{diag}} = \tilde{\Phi}_{\{\mathrm{SD},1\}}^{*\mathrm{diag}}$ and $\tilde{\Phi}_{\{\mathrm{SR},2\}}^{\mathrm{diag}} = \tilde{\Phi}_{\{\mathrm{SR},1\}}^{*\mathrm{diag}}$ which makes effective channel matrix orthogonal. After ignoring interference, (14) can be written as

$$\mathbf{y} \stackrel{\mathrm{def}}{=} \begin{bmatrix} \mathbf{F}\bar{\mathbf{r}}_{\mathrm{D}}^j \\ \mathbf{F}\mathbf{P}\bar{\mathbf{r}}_{\mathrm{D}}^{*j+1} \end{bmatrix} = \underbrace{\begin{bmatrix} \Delta_1^{\mathrm{diag}} & \Delta_2 \\ \Delta_2^* & -\Delta_1^{*,\mathrm{diag}} \end{bmatrix}}_{\Delta} \begin{bmatrix} \mathbf{F}\mathbf{x}_1^j(n) \\ \mathbf{F}\mathbf{x}_2^j(n) \end{bmatrix} + \begin{bmatrix} \mathbf{F}\mathbf{w}_{\mathrm{D}}^j \\ \mathbf{F}\mathbf{P}\mathbf{w}_{\mathrm{D}}^{*j+1}) \end{bmatrix}, \tag{15}$$

where $\Delta_1^{\mathrm{diag}} = \tilde{\Phi}_{\mathrm{SD}}^{H,\mathrm{diag}}\tilde{\mathbf{D}}_{\mathrm{RD}}\tilde{\Phi}_{\mathrm{SR}}^{\mathrm{diag}}\tilde{\mathbf{D}}_{\mathrm{SR}}$, $\Delta_2 = \tilde{\mathbf{D}}_\tau\mathbf{D}_{\mathrm{SD}}$. Note that for notational simplicity ρ is being embedded into the Δ_1^{diag} matrix.

Since Δ is an orthogonal matrix, we can (without loss of optimality) multiply both sides of (15) by Δ^* to decouple the two signals $\mathbf{x}_1^j(n)$ and $\mathbf{x}_2^j(n)$ resulting in

$$\tilde{\mathbf{y}} \stackrel{\mathrm{def}}{=} \Delta^*\mathbf{y} = \begin{bmatrix} \tilde{\Delta} & 0 \\ 0 & \tilde{\Delta} \end{bmatrix} \begin{bmatrix} \mathbf{x}_1^j(n) \\ \mathbf{x}_2^j(n) \end{bmatrix} + \Delta^* \begin{bmatrix} \mathbf{F}\mathbf{w}_{\mathrm{D}}^j \\ \mathbf{F}\mathbf{P}\mathbf{w}_{\mathrm{D}}^{*j+1}) \end{bmatrix}, \tag{16}$$

where the resulting noise is still white, and $\tilde{\Delta} \stackrel{\mathrm{def}}{=} |\Delta_1|^2 + |\Delta_2|^2$ is an $M \times M$ diagonal matrix with (i,i) elements equal to $|\rho\Delta_1(i,i)|^2 + |\Delta_2(i,i)|^2$ which also equals to the sum of the square of the i^{th} discrete Fourier transform (DFT) coefficient of the first and the second CIR's. The filtered noise vector has a diagonal auto-correlation matrix equal to $\mathrm{diag}(\tilde{\Delta}, \tilde{\Delta})$. Therefore, the MMSE-FDE is represented by $M \times M$ diagonal matrix whose (i,i) element is given by

$$\mathbf{W}(i,i) = \frac{\Delta^*(i,i)}{|\Delta(i,i)|^2 + \frac{1}{SNR}}, \tag{17}$$

where signal to noise ratio (SNR) $\stackrel{\mathrm{def}}{=} \sigma_x^2/\sigma_n^2$. The output of the MMSE-FDE denoted by $\mathbf{r} = \mathbf{W}\tilde{\mathbf{y}}$, is transformed back to time domain followed by the estimate of $\mathbf{x}_1^j(n)$ and $\mathbf{x}_2^j(n)$.

In the second stage of equalization, equalizer perform CPR and residual ISI cancelation, which equalizes the channel matrix in (12) and (13). Since $\mathbf{H}_{\mathrm{SD}}$ is not a circulant matrix, use the estimate of $\mathbf{x}_1^j(n)$ and $\mathbf{x}_2^j(n)$ to make $\mathbf{H}_{\mathrm{SD}}$ approximately equal to $\tilde{\mathbf{H}}_{\mathrm{SD}}$. Also, the residual ISI is canceled by using the estimate of $\mathbf{x}_1^j(n)$ and $\mathbf{x}_2^j(n)$,

$$\begin{aligned} \check{\mathbf{r}}_{\mathrm{D}}^j &= \tilde{\mathbf{H}}_{\mathrm{RD}}\tilde{\Gamma}_{\mathrm{SR}}\tilde{\mathbf{H}}_{\mathrm{SR}}\mathbf{x}_1^j(n) + \tilde{\mathbf{R}}_\tau\mathbf{H}_{\mathrm{SD}}\mathbf{x}_2^j(n) \\ &\quad + \underbrace{\tilde{\mathbf{R}}_\tau\mathbf{C}_{\mathrm{SD}}\hat{\mathbf{x}}_2^j(n)}_{\text{CPR}} - \underbrace{\mathbf{F}^H\Delta_1^{\mathrm{non-diag}}\mathbf{F}\hat{\mathbf{x}}_1^j(n)}_{\text{RISI}} + \bar{\mathbf{w}}_{\mathrm{D}}^j, \\ &= \tilde{\mathbf{H}}_{\mathrm{RD}}\tilde{\Gamma}_{\mathrm{SR}}\tilde{\mathbf{H}}_{\mathrm{SR}}\mathbf{x}_1^j(n) + \tilde{\mathbf{R}}_\tau\tilde{\mathbf{H}}_{\mathrm{SD}}\mathbf{x}_2^j(n) \\ &\quad - \mathbf{F}^H\Delta_1^{\mathrm{non-diag}}\mathbf{F}\tilde{\mathbf{x}}_1^j(n) + \bar{\mathbf{w}}_{\mathrm{D}}^j, \end{aligned} \tag{18}$$

$$\begin{aligned} \check{\mathbf{r}}_{\mathrm{D}}^{j+1} &= -\tilde{\mathbf{H}}_{\mathrm{RD}}\tilde{\Gamma}_{\mathrm{SR}}\tilde{\mathbf{H}}_{\mathrm{SR}}\mathbf{P}\mathbf{x}_2^{*j}(n) + \tilde{\mathbf{R}}_\tau\mathbf{H}_{\mathrm{SD}}\mathbf{P}\mathbf{x}_1^{*j}(n) \\ &\quad + \underbrace{\tilde{\mathbf{R}}_\tau\mathbf{C}_{\mathrm{SD}}\mathbf{P}\hat{\mathbf{x}}_1^{*j}(n)}_{\text{CPR}} + \underbrace{\mathbf{F}^H\Delta_1^{\mathrm{non-diag}}\mathbf{F}\mathbf{P}\hat{\mathbf{x}}_1^j(n)}_{\text{RISI}} + \bar{\mathbf{w}}_{\mathrm{D}}^{j+1}, \\ &= -\tilde{\mathbf{H}}_{\mathrm{RD}}\tilde{\Gamma}_{\mathrm{SR}}\tilde{\mathbf{H}}_{\mathrm{SR}}\mathbf{P}\mathbf{x}_2^{*j}(n) + \tilde{\mathbf{R}}_\tau\tilde{\mathbf{H}}_{\mathrm{SD}}\mathbf{P}\mathbf{x}_1^{*j}(n) \\ &\quad + \mathbf{F}^H\Delta_1^{\mathrm{non-diag}}\mathbf{F}\mathbf{P}\hat{\mathbf{x}}_1^j(n) + \bar{\mathbf{w}}_{\mathrm{D}}^{j+1}, \end{aligned} \tag{19}$$

where $\mathbf{C}_{\mathrm{SD}} \in \mathbb{C}^{M\times M}$ such that $\tilde{\mathbf{H}}_{\mathrm{SD}} = \mathbf{H}_{\mathrm{SD}} + \mathbf{C}_{\mathrm{SD}}$.

Eqs. (18) and (19) are similar to (12) and (13). So performing the same processing as was done for (12) and (13) yields a better estimate of $\mathbf{x}_1^j(n)$ and $\mathbf{x}_2^j(n)$.

IV. Simulation Results

For simulation parameters, consider turbo coded systems with code rate = 3/4, PUSCH data symbol size of $M = 512$, QPSK, 16-QAM, 64-QAM, 5 MHz bandwidth and 7.68 MHz sampling frequency. All the underlying links experience frequency selective fading channels and are modeled as Pedestrian B and Typical Urban (TU) [23] with Rayleigh fading having exponential power delay profile. Assume that the channel is known to the receiver.

Fig. 4 compares the bit error rate (BER) versus SNR when only TO is present in the system. Simulation is performed for the code rates of 3/4 with QPSK, 16-QAM and 64-QAM. The proposed equalizer yields a significant gain for 64-QAM modulation at the BER = 10^{-3}. For the case of 16-QAM a gain of 1.5dB at the BER = 10^{-3} is obtained. Small gain of 0.3dB is obtained for QPSK. Effectively TO does not have significant impact on the system performance if the order of the modulation scheme is low. However, it has severe impact

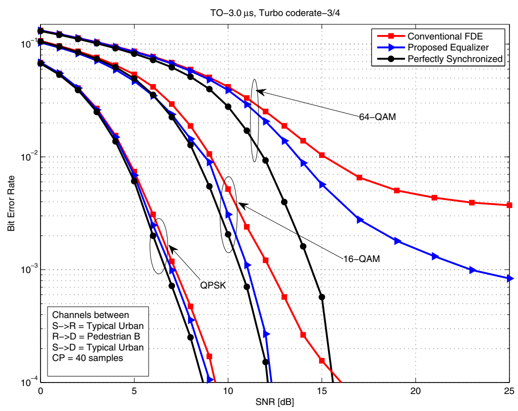

Fig. 4. BER vs SNR for coded system with and without timing offset.

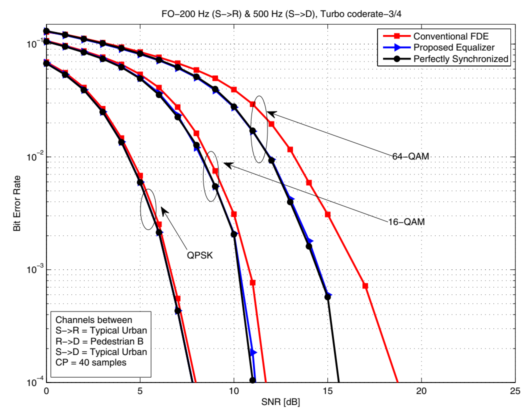

Fig. 6. BER vs SNR for coded system with and without carrier frequency offset, with source velocity of 200 km/h.

on the higher order modulation and on the uncoded system [10] and on the coded system with high code rate.

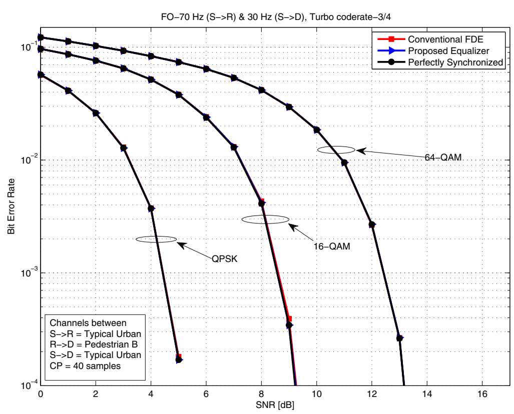

Fig. 5. BER vs SNR for coded system with and without carrier frequency offset, with source velocity of 30 km/h.

Fig. 5 and Fig. 6 compares the BER versus SNR when only CFOs are present in the system with QPSK, 16-QAM and 64-QAM. System performance does not have any impact due to low CFOs (source terminal is moving with the velocity equal to or lesser than 30 km/h) as shown in Fig. 5. With the source velocity at 200 km/h, the system performance is degraded for the higher order modulations, but the proposed equalizer is able to compensate the high CFOs caused due to the source mobility as shown in Fig. 6. It is observed that system does not have severe impact of low CFOs, but it cannot tolerate large CFOs as in 16-QAM and 64-QAM. For 64-QAM, there is 2.5dB gain at BER = 10^{-3} using proposed equalizer. Therefore, the proposed equalizer plays a significant role in improving the system performance.

Fig. 7 shows the performance of a single-user DSTBC SC MMSE-FDE coded system. Under the presence of TO and CFOs simultaneously, relay based system performance degrades significantly. Under the assumption that TO and CFOs are unknown to receiver, BER degrades because of IBI effect and symbols interference due to CFOs. The case where the perfect estimates of TO and CFOs are known to the receiver, system performance improves significantly at the BER = 10^{-3} using the proposed equalizer. In practice, perfect estimates of TO and CFOs are rarely possible, so performance degrades as estimator error variance increases. We have considered the case, where only CFOs have imperfect estimates. CFO estimator error variance is Gaussian distributed [24] with mean zero and some variance σ_f^2. Fig. 7 also shows the performance between perfect estimation ($\sigma_f = 0$) and imperfect estimations with error variance ($\sigma_f = 10\sigma_n$ and $15\sigma_n$). It is observed that the proposed equalizer can also tolerate the presence of small estimation errors.

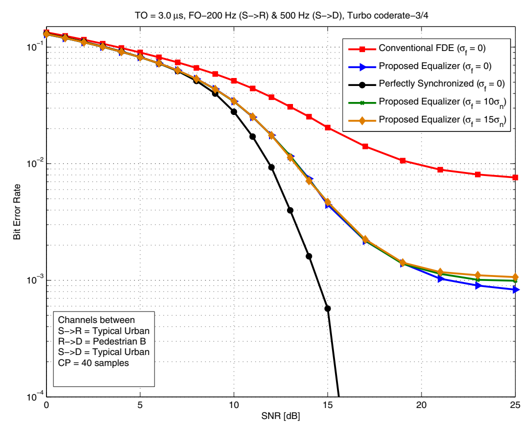

Fig. 7. BER vs. SNR with and without timing and frequency errors with perfect and imperfect estimation of frequency offsets.

V. Conclusion

This paper discussed the effect of simultaneous presence of timing offsets and carrier frequency offsets in a relay based SC MMSE-FDE system. The proposed two stage technique to combat the problem, has been constructed on top of the 3GPP LTE uplink standard. The presence of TOs and CFOs does not have a severe impact on the system performance if the source has low velocity and lower order modulation. At high velocity and higher order modulation, system performance degrades and the proposed equalizer improves the performance significantly, without increasing the complexity at the receiver. Simulation results show that the proposed technique of interblock interference cancelation, residual intersymbol interference cancelation and CP reconstruction, gracefully combat time and frequency offsets in DSTBC SC MMSE-FDE transmission scheme.

Appendix: Derivation of (14)

Take (12) and multiply both side by $\tilde{\Gamma}_{\mathrm{SD}}^H$,

$$\tilde{\Gamma}_{\mathrm{SD}}^H \mathbf{r}_{\mathrm{D}}^j = \rho \tilde{\Gamma}_{\mathrm{SD}}^H \tilde{\mathbf{H}}_{\mathrm{RD}} \tilde{\Gamma}_{\mathrm{SR}} \tilde{\mathbf{H}}_{\mathrm{SR}} \mathbf{x}_1^j(n) + \tilde{\mathbf{R}}_\tau \tilde{\mathbf{H}}_{\mathrm{SD}} \mathbf{x}_2^j(n) + \tilde{\Gamma}_{\mathrm{SD}}^H \mathbf{w}_{\mathrm{D}}^j, \tag{20}$$

now using *P1*, and taking FFT both side, we get

$$\mathbf{R}_{\mathrm{D}}^j = \rho \tilde{\Phi}_{\mathrm{SD},1}^H \tilde{\mathbf{D}}_{\mathrm{RD}} \tilde{\Phi}_{\mathrm{SR},1} \tilde{\mathbf{D}}_{\mathrm{SR}} \mathbf{F} \mathbf{x}_1^j(n) + \tilde{\mathbf{D}}_\tau \tilde{\mathbf{D}}_{\mathrm{SD}} \mathbf{F} \mathbf{x}_2^j(n) + \mathbf{W}_{\mathrm{D}}^j, \tag{21}$$

where $\tilde{\Phi}_{\mathrm{SR},1} = \mathbf{F}_{\mathrm{M}} \tilde{\Gamma}_{\mathrm{SR}}^H \mathbf{F}_{\mathrm{M}}^H$ and $\tilde{\Phi}_{\mathrm{SD},1} = \mathbf{F}_{\mathrm{M}} \tilde{\Gamma}_{\mathrm{SD}} \mathbf{F}_{\mathrm{M}}^H$ are non-diagonal matrices.

Take (13), conjugate both side and multiplying both side by $\tilde{\Gamma}_{\mathrm{SD}}^T$, we get,

$$\begin{aligned}\tilde{\Gamma}_{\mathrm{SD}}^T \bar{\mathbf{r}}_{\mathrm{D}}^{*j+1} &= -\rho \tilde{\Gamma}_{\mathrm{SD}}^T \tilde{\mathbf{H}}_{\mathrm{RD}}^* \tilde{\Gamma}_{\mathrm{SR}}^* \tilde{\mathbf{H}}_{\mathrm{SR}}^* \mathbf{P} \mathbf{x}_2^j(n) + \tilde{\mathbf{R}}_\tau^* \mathbf{H}_{\mathrm{SD}}^* \mathbf{P} \mathbf{x}_1^j(n) \\ &\quad + \tilde{\Gamma}_{\mathrm{SD}}^T \mathbf{w}_{\mathrm{D}}^{*j+1}. \end{aligned} \tag{22}$$

now multiply both side by $\mathbf{P}$, use identity $\mathbf{PP} = \mathbf{I}$ and using *P2*, we get,

$$\begin{aligned}\mathbf{P} \tilde{\Gamma}_{\mathrm{SD}}^T \bar{\mathbf{r}}_{\mathrm{D}}^{*j+1} &= -\rho \mathbf{P} \tilde{\Gamma}_{\mathrm{SD}}^T \mathbf{P} \tilde{\mathbf{H}}_{\mathrm{RD}}^H \mathbf{P} \tilde{\Gamma}_{\mathrm{SR}}^H \mathbf{P} \tilde{\mathbf{H}}_{\mathrm{SR}}^H \tilde{\Gamma}_{\mathrm{SD}} \mathbf{x}_2^j(n) \\ &\quad + \tilde{\mathbf{R}}_\tau^H \mathbf{H}_{\mathrm{SD}}^H \mathbf{x}_1^j(n) + \tilde{\Gamma}_{\mathrm{SD}} \mathbf{P} \mathbf{w}_{\mathrm{D}}^{*j+1}. \end{aligned} \tag{23}$$

Note that $\mathbf{H}_{\mathrm{SD}}$ is not a circulant matrix, and, therefore, it is not possible to use MMSE-FDE, but to keep receiver complexity minimal and to perform MMSE-FDE we have used $\check{\mathbf{H}}_{\mathrm{SD}}$ instead of $\mathbf{H}_{\mathrm{SD}}$ in (23).

Applying *P1* and taking FFT both side on (23), we get

$$\mathbf{R}_{\mathrm{D}}^{j+1} = -\rho \tilde{\Phi}_{\mathrm{SD},2} \tilde{\mathbf{D}}_{\mathrm{RD}}^* \tilde{\Phi}_{\mathrm{SR},2} \tilde{\mathbf{D}}_{\mathrm{SR}}^* \mathbf{F} \mathbf{x}_2^j(n) + \tilde{\mathbf{D}}_{\mathrm{SD}}^* \tilde{\mathbf{D}}_\tau^* \mathbf{F} \mathbf{x}_1^j(n) + \mathbf{W}_{\mathrm{D}}^j, \tag{24}$$

where $\tilde{\Phi}_{\mathrm{SR},2} = \mathbf{F}_{\mathrm{M}} \mathbf{P} \tilde{\Gamma}_{\mathrm{SR}}^* \mathbf{P} \mathbf{F}_{\mathrm{M}}^H$ and $\tilde{\Phi}_{\mathrm{SD},2} = \mathbf{F}_{\mathrm{M}} \mathbf{P} \tilde{\Gamma}_{\mathrm{SD}}^T \mathbf{P} \mathbf{F}_{\mathrm{M}}^H$ are non-diagonal matrices.

References

[1] 3rd Generation Partnership Project (3GPP); Technical Specification Group Radio Access Network, "Evolved universal terrestrial radio access (e-utra); Physical Channels and Modulation (3GPP TS 36.211 Ver. 8.2.0 (2008-03)(Release 8));," 3rd Generation Partnership Project (3GPP), Tech. Rep., 2008.

[2] D. Falconer, S. Ariyavisitakul, A. Benyamin-Seeyar, and B. Eidson, "Frequency domain equalization for single-carrier broadband wireless systems," *IEEE Commun. Mag.*, vol. 40, no. 4, pp. 58–66, 2002.

[3] M. Clark, "Adaptive frequency-domain equalization and diversity combining for broadband wireless communications," *IEEE J. Select. Areas Commun.*, vol. 16, no. 8, pp. 1385–1395, Oct. 1998.

[4] H. Sari, G. Karam, and I. Jeanclaude, "Transmission techniques for digital terrestrial tv broadcasting," *IEEE Commun. Mag.*, vol. 33, no. 2, pp. 100–109, Feb. 1995.

[5] S. Alamouti, "A simple transmit diversity technique for wireless communications," *IEEE J. Select. Areas Commun.*, vol. 16, no. 8, pp. 1451–1458, Oct 1998.

[6] J. N. Laneman and G. W. Wornell, "Distributed space–time–coded protocols for exploiting cooperative diversity in wireless networks," *IEEE Trans. Inform. Theory*, vol. 49, no. 10, pp. 2415–2425, Oct. 2003.

[7] A. Sendonaris, E. Erkip, and B. Aazhang, "User cooperation diversity I & II," *IEEE Trans. Commun.*, vol. 51, no. 11, pp. 1927–1948, Nov. 2003.

[8] X. Li and N. Wu, "Power efficient wireless sensor networks with distributed transmission-induced space spreading," in *Proc. Annual Asilomar Conf. Signals, Syst., Comp.*, vol. 2, Pacific Grove, California, Oct. 30 –Nov. 2 2003, pp. 1698–1702.

[9] H. Mheidat, M. Uysal, and N. Al-Dhahir, "Equalization techniques for distributed space-time block codes with amplify-and-forward relaying," *IEEE Trans. Signal Processing*, vol. 55, no. 5, pp. 1839–1852, May 2007.

[10] A. Yadav, M. Juntti, and J. Karjalanen, "Combating timing asynchronism in relay transmission for 3GPP LTE uplink," in *Proc. IEEE Wireless Commun. and Networking Conf.*, Budapest, Hungary, Apr. 05–08 2009, pp. 1–6.

[11] I. Brown, D.R., G. Prince, and J. McNeill, "A method for carrier frequency and phase synchronization of two autonomous cooperative transmitters," in *Proc. IEEE Works. on Sign. Proc. Adv. in Wirel. Comms.*, New York, NY USA, June 5–8 2005, pp. 260–264.

[12] G. Barriac, R. Mudumbai, and U. Madhow, "Distributed beamforming for information transfer in sensor networks," in *Proc. IEEE Int. Symp. on Inform. Proc. in Sensor Networks*, Berkeley, CA USA, Apr. 26–27 2004, pp. 81–88.

[13] Y.-S. Tu and G. Pottie, "Coherent cooperative transmission from multiple adjacent antennas to a distant stationary antenna through AWGN channels," in *Proc. IEEE Veh. Technol. Conf.*, vol. 1, Birmingham, Alabama USA, May 6–9 2002, pp. 130–134.

[14] H.-Y. Shen, H. Yang, B. Sikdar, and S. Kalyanaraman, "A distributed system for cooperative MIMO transmissions," in *Proc. IEEE Global Telecommun. Conf.*, vol. 1, New Orleans, Louisiana USA, Nov. 30 – Dec. 4 2008, pp. 1–5.

[15] D. Veronesi and D. Goeckel, "Multiple frequency offset compensation in cooperative wireless systems," in *Proc. IEEE Global Telecommun. Conf.*, San Francisco, CA USA, Nov. 27 –Dec. 1 2006, pp. 1–5.

[16] A. O. Yilmaz, "Cooperative diversity in carrier frequenct offset," *IEEE Commun. Lett.*, vol. 11, no. 4, pp. 307–309, Apr. 2007.

[17] M. R. Bhatnagar, A. Hjorungnes, and L. Song, "Cooperative communications over flat fading channels with carrier offsets: A double-differential modulation approach," *EURASIP Journal on Advances in Signal Processing*, vol. 2008, Article ID 531786, 11 pages, 2008. doi:10.1155/2008/531786.

[18] Y. Zhang and J. Zhang, "Multiple CFOs compensation and BER analysis for cooperative communication systems," in *Proc. IEEE Wireless Commun. and Networking Conf.*, Budapest, Hungary, Apr. 05–08 2009, pp. 1–6.

[19] P. Herhold, E. Zimmermann, and G. Fettweis, "On the performance of cooperative amplify-and-forward relay networks," *European Trans. Telecommun.*, vol. 16, Oct. 2004.

[20] R. Nabar and H. Bolcskei, "Space-time signal design for fading relay channels," in *Proc. IEEE Global Telecommun. Conf.*, vol. 4, San Frasncisco, CA USA, Dec. 1–5 2003, pp. 1952–1956.

[21] R. Nabar, H. Bolcskei, and F. Kneubuhler, "Fading relay channels: performance limits and space-time signal design," *IEEE J. Select. Areas Commun.*, vol. 22, no. 6, pp. 1099–1109, Aug. 2004.

[22] S. Zhou and G. B. Giannakis, "Space-time coding with maximum diversity gains over frequency-selective fading channels," *IEEE Signal Processing Lett.*, vol. 8, no. 10, pp. 269–272, Oct. 2001.

[23] 3rd Generation Partnership Project (3GPP); Technical Specification Group Radio Access Network, "Evolved universal terrestrial radio access (e-utra); user equipment (ue) radio transmission and reception (3GPP TS 36.101 Ver. 8.0.0 (2007-12) (Release 8))," 3rd Generation Partnership Project (3GPP), Tech. Rep., 2007.

[24] P. Parker, P. Mitran, D. Bliss, and V. Tarokh, "On bounds and algorithms for frequency synchronization for collaborative communication systems," *IEEE Trans. Signal Processing*, vol. 56, no. 8, pp. 3742–3752, Aug. 2008.